Hindawi
Geofluids
Volume 2022, Article ID 4858395, 11 pages
https://doi.org/10.1155/2022/4858395

Research Article

Experimental Study on the Aeolian Sand Solidification via MICP Technique

Yijun Zhou[1] **and Yulong Chen**[2]

[1]*College of Civil Engineering, North China University of Science and Technology, Tangshan, China*
[2]*School of Energy and Mining Engineering, China University of Mining and Technology, Beijing 100083, China*

Correspondence should be addressed to Yijun Zhou; zyjfcb@126.com

Received 24 February 2022; Accepted 19 April 2022; Published 11 May 2022

Academic Editor: Wen-long Shen

This study solidifies the aeolian sand by microbial-induced carbonate precipitation (MICP) technique. The effects of cementation solution with different concentrations, particle size, and grouting batches are examined via the bender element, unconfined compressive test, and scanning electron microscope (SEM). The bender element results show that the wave speed of loose aeolian sand is 200 m/s; however, after solidification of the aeolian sand, the speed of P-wave is about 450-600 m/s and S-wave is about 350-500 m/s. Additionally, the unconfined compressive strength (UCS) results indicate that when the concentration of cementation solution is 0.75 mol/L, the UCS of biosolidified sand sample is the highest. Then, compared with the aeolian sand with original grade, the particles ranging from 0.1 to 0.4 mm have a better cementation effect. Moreover, the UCS of biosolidified sand samples increases along with the grouting batch. From the SEM images, it can be seen that when the grouting batch reaches to five times, the particles are almost completely covered by $CaCO_3$ crystals compared with the three batches and four batches.

1. Introduction

The mechanism MICP is that the urease produced by microorganisms and the ammonia gas and carbon dioxide produced by the hydrolysis of urea can be converted into ammonium ion and bicarbonate ion in the alkaline solution environment. Then, the bicarbonate ion will attract calcium ions in solution thus precipitating calcium carbonate. Moreover, as reported, the microorganism is generally negatively charged thereby absorbing positively charged cations such as calcium ions, making the microorganism become the crystal nucleus in the crystallization process of calcium carbonate.

The researchers realized the importance of microbial mineralization as early as 1970s [1, 2]. The researchers studied on the urease activity of bacteria as the research object and study the effects of nickel ions, grouting methods, and different calcium salt concentrations on the strength of microbial grouting solidified sands [3, 4]. Researchers found that the concentration of nutrients is negatively correlated with the strength of the sample. When the concentration is low, the strength of the sample is higher and the sample integrity is better [5]. Scholars in the United Kingdom have discovered through research that step-by-step grouting can improve the uniformity of calcium carbonate spatial distribution. The calcium carbonate generated in the early and midterm will help to fix the microorganisms and induce the formation of new calcium carbonate [6]. The research team in Saudi Arabia discussed the influence of culture medium, bacterial concentration, and different buffers on the compressive strength of cement mortar. The strength can reach up to 39.6 MPa [7]. Researchers found that when the particle size distribution contains 75% coarse aggregate and 25% fine aggregate, the maximum uniaxial compressive strength is about 575 kPa. Adding fine aggregate to the coarse aggregate can reduce the size of the coarse aggregate particles. Provide more bridge contact [8, 9].

Ivanov and Chu applied MICP technology to plugging and improving soil strength in geotechnical engineering

Table 1: Test on natural moisture content of aeolian sand.

Number	Quality of wet sands (g)	Quality of dry sands (g)	Quality of water (g)	Moisture content (%)	Average of moisture content (%)
1	15.98	15.85	0.13	0.82	0.8
2	19.31	19.16	0.15	0.78	

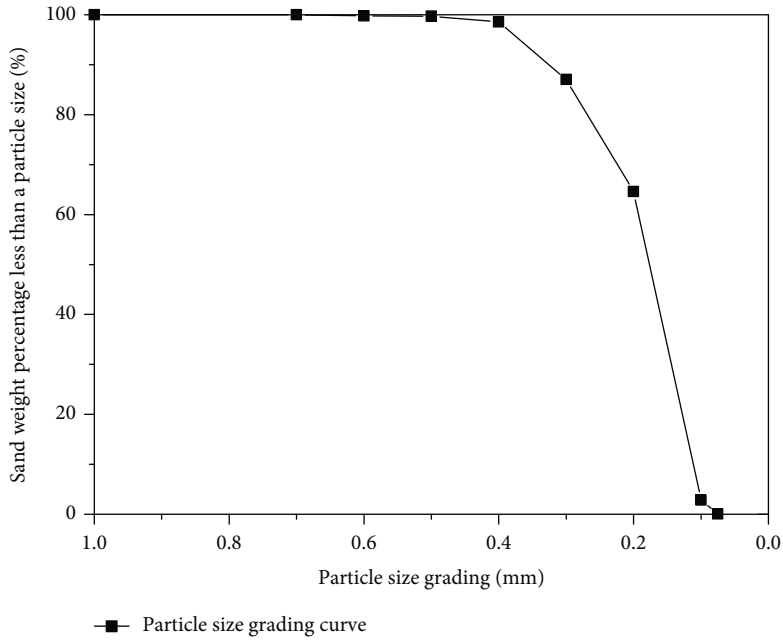

Figure 1: Particle size distribution of aeolian sand.

Table 2: Aeolian sand particle size distribution.

Size (mm)	<0.075	<0.1	<0.2	<0.3	<0.4	<0.5	<0.6	<0.7	<1
Percentage (%)	0.055	2.807	64.583	87.067	98.542	99.733	99.768	100	100

[10]. Harkes et al. optimized the MICP grouting technology by the clogging of the grouting port and the unevenness of the sample solidification that often occurred in the experiment [11]. Dejong et al. used microbial solidification to gel the concrete and monitored the shear wave velocity during the repair process [12]. The researchers in Canada successfully reduced the permeability of oilfield sandstone by cementing sandstone particles [13]. Some of the research teams used spraying, immersion, and infiltration methods to conduct indoor or on-site microbial coating tests on limestone, marble, and sandstone stone samples or actual cultural relics [14–19].

Some scholars have also pay attention to how to improve the economy of the MICP [20]. And other scholars began to pay attention to adding some other additives to improve the strength of MICP. For instance, Dhami et al. and Choi et al. added polyvinyl alcohol fiber and found that the UCS and splitting tensile strength of the sample were increased by 138% and 186%, respectively, and the permeability was reduced by 126% [21, 22]. Xu et al. found that the uniaxial compressive performance of the MICP-treated sand column has been improved by adding magnesium ions [23]. Cheng and Cord-Ruwisch tried the surface infiltration method and compared it with the continuous grouting method [24].

Another scholars have studied the MICP by the numerical simulation. The research team in the Netherlands has established a complete mathematical model of the microbial grouting process [25–27]. The Swiss Federal Institute of Technology established a model to consider the coupling of various factors, including biology, chemistry, fluids, and mechanics [28]. The research team used the three-dimensional discrete element method (DEM) to simulate the mechanical behavior of siltstone after MICP reinforcement [29]. Cheng et al. use CT scanning technology to quantify the key microscopic properties of MICP, such as the size of crystals [30].

The model tests are of great help to MICP research [31–33]. In 2010, scholars in the Netherlands applied the technology of microbial induction to generate calcium carbonate in the on-site sandy gravel soil reinforcement project [34, 35]. Van Paassen et al. used microbiological methods to carry out 1 m^3 and 100 m^3 sand samples for prototype sand foundation reinforcement tests [36]. Kalkan analyzed the reinforcement mechanism and influencing factors of MCP [37].

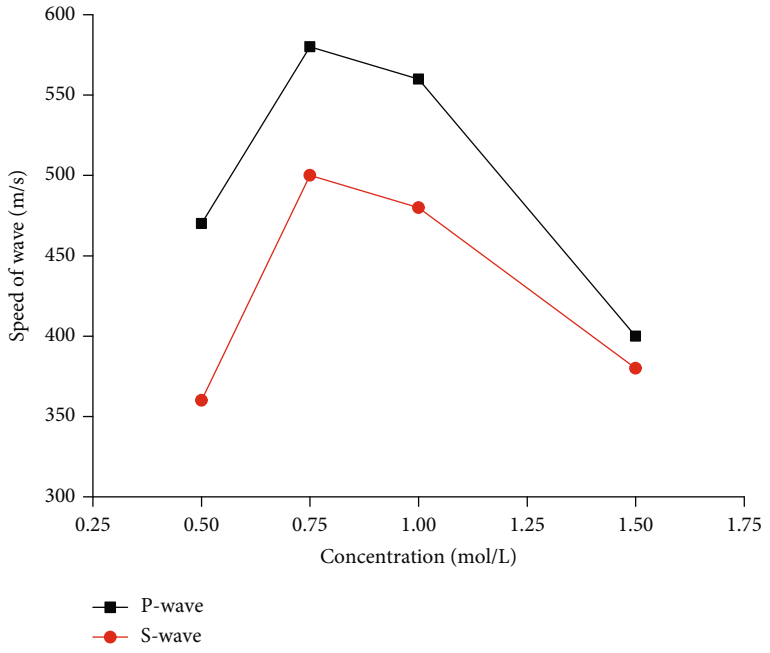

Figure 2: The wave speed of different nutrient concentrations.

Table 3: Experimental scheme.

Fixation solution	Concentration of fixation solution (mmol/L)	Cementation solution	Concentration of cementation solution (mol/L)	Particle size distribution	Grouting batches
$CaCl_2$	25	$CaCl_2 + CH_4N_2O$	0.25	Particles all size/particle size in 0.1-0.4mm	3 times
	50		0.5		4 times
	75		0.75		5 times
	100		1.0		
	150		1.5		

Note: the black font in Table 3 represents the basic plan.

(a) Big probe (b) Small probe

Figure 3: Bender element.

In summary, some research results have been made in the MICP technique for solidifying various saturated sand and unsaturated sands, including metallogenic mechanism of sand, grouting reinforcement method, and nutrient concentration for the effect of mineralization. However, the aeolian sand is different from the solidifying various saturated sands

(a) (b)

Figure 4: The process of testing the bender element.

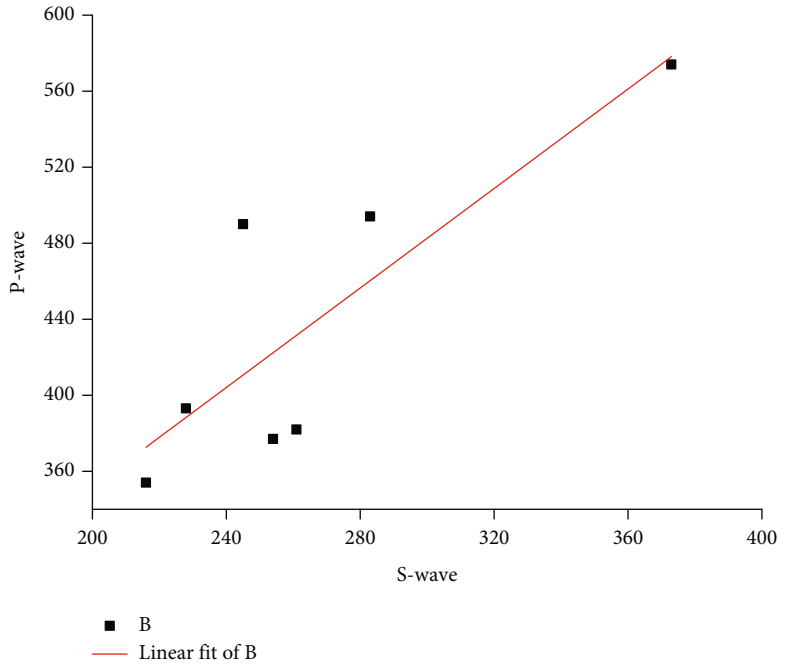

Figure 5: Curve fitting of P-S wave.

as well as unsaturated sand, because of the much lower moisture content and the much poorer particle size distribution. Meanwhile, there is no effect on solidifying aeolian sand by using the traditional foundation reinforcement methods. In addition, there are few researches on the MICP for aeolian sand solidification. Therefore, it is very necessary to carry out research on aeolian sand solidification via MICP.

2. Materials and Methods

2.1. Materials

2.1.1. Aeolian Sand Selection. The aeolian sand used in the current study was sampled (0.3 m below the ground surface) from the Kubuqi Desert, China (latitude: 40.46212, longitude: 108.653344), which is the ninth largest desert in the world and the sixth largest in China. Due to physical weathering and chemical weathering, the aeolian sand particles are angular, weak in strength, and uneven in size distribution and contain a certain amount of fine soil particles.

2.1.2. Physical Properties of Aeolian Sand

(1) Natural Moisture Content Calculation. According to GB/T50123-1999 geotechnical test standards of China, the natural moisture content test needs to be carried out twice and its arithmetic average is taken. The formula of natural moisture content for aeolian sand is as follows:

$$\mathrm{Wo} = \left(\frac{\mathrm{m0}}{\mathrm{md}} - 1\right) \times 100\%. \quad (1)$$

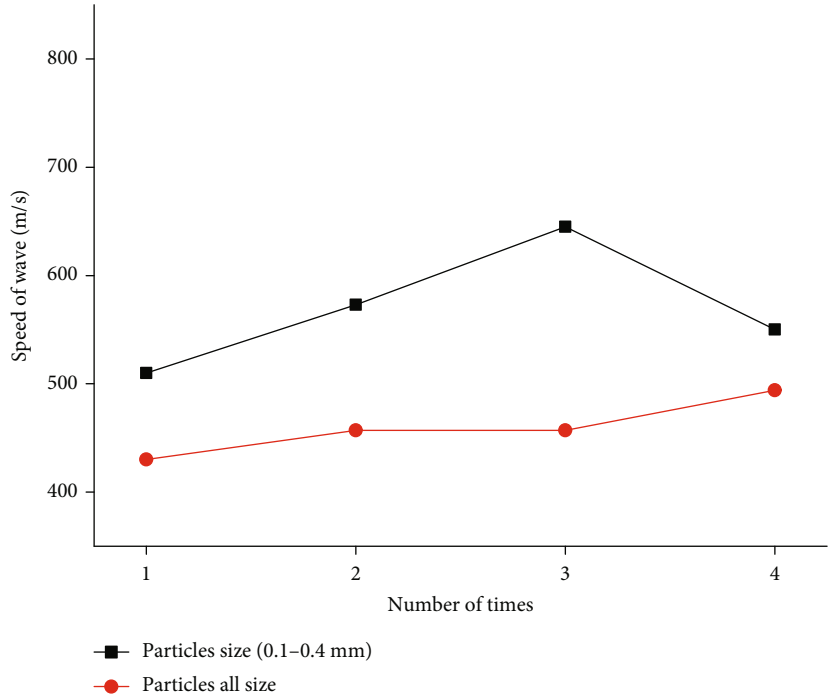

Figure 6: The wave speed for 1 mol/L.

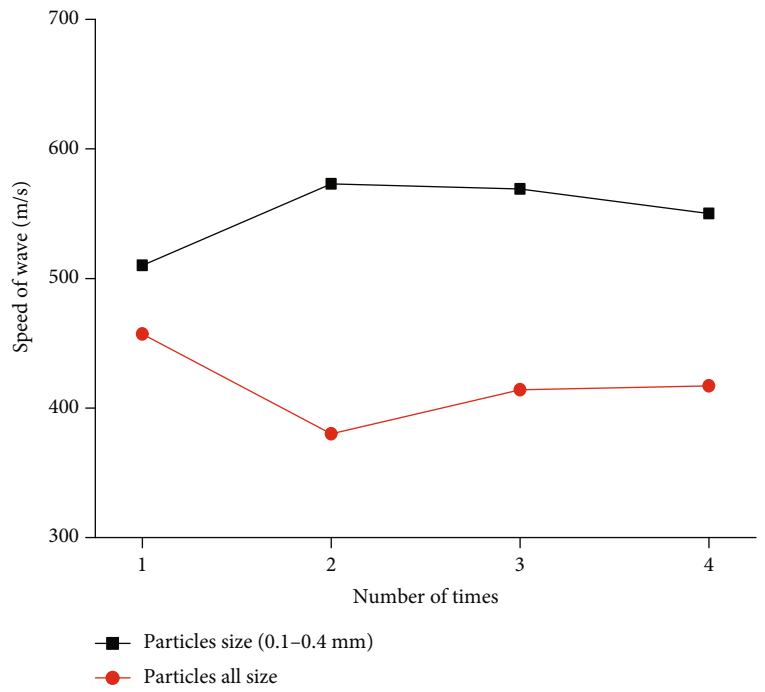

Figure 7: The wave speed for 1.5 mol/L.

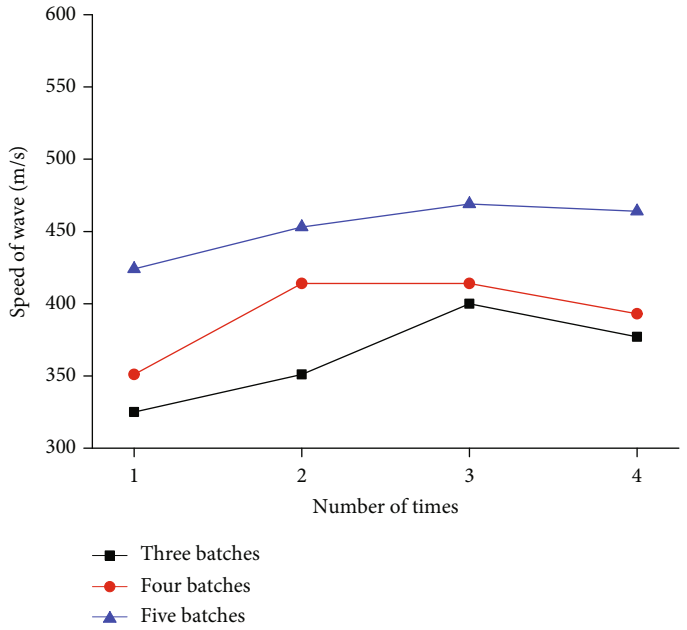

(a) Nutrient of 0.5 mol/L

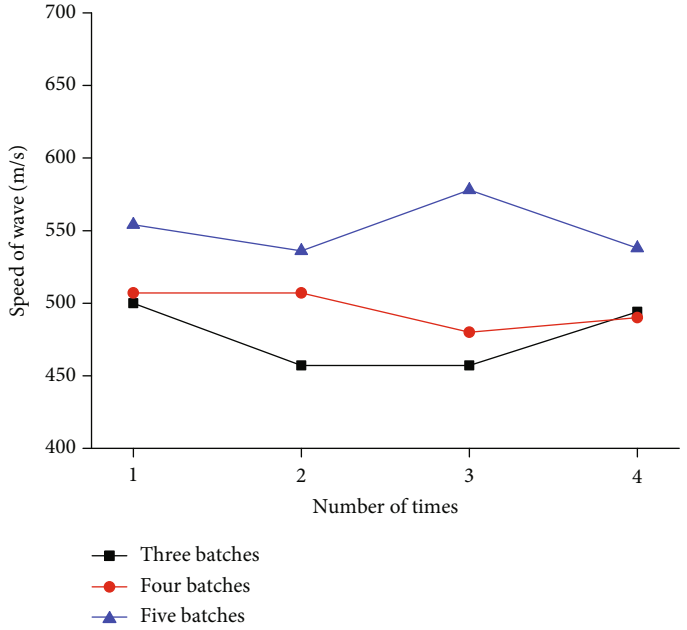

(b) Nutrient of 0.75 mol/L

Figure 8: Continued.

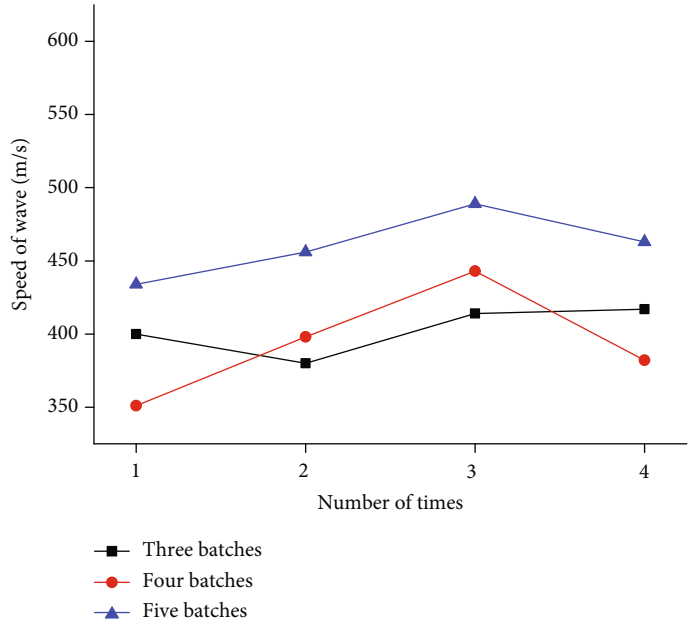

(c) Nutrient of 1 mol/L

Figure 8: Comparison chart of wave speed for different grouting batches.

m0 is the quality of wet soil (g), and md is the quality of dry soil (g). The testing results of natural moisture content of aeolian sand are shown in Table 1. The natural moisture content of aeolian sand is about 0.80% by calculation.

(2) Particle Size Distribution Analysis. The particle size distribution is presented in Figure 1. As can be seen in Table 2, the particle size distribution of the aeolian sand is mainly between 0.1 mm and 0.4 mm.

According to Figure 1, the particle size distribution of the aeolian sand is mainly between 0.1 mm and 0.4 mm. Additionally, the effective particle is $d_{10} = 0.11$, the median is $d_{50} = 0.17$, and the limit particle size is $d_{60} = 0.19$ and $d_{30} = 0.14$. The uneven coefficient of aeolian sand is $C_u = d_{60}/d_{10} = 1.73$; and the curvature coefficient is $C_C = {d_{30}}^2/(d_{60} \times d_{10}) = 0.74$.

According to GB/T50123-1999 geotechnical test standards of China, the pH value of suspension water of aeolian sand is 8.77.

2.1.3. Bacteria. The microbe used in the current study is Sporosarcina pasteurii, which has a strong survivability as well as a high urease production ability. The cell surface is negatively charged, the spores are oval or spherical, and the cell rod is 2-3 μm long and 1-2 μm in diameter. The process of bacterial culture is presented in Figure 2 [23]. The average urease activity is about 15.01 mmol/min, and the average OD600 = 2.62.

2.1.4. Fixation and Cementation Solution. The cementation solution herein is composed of $CaCl_2$ and urea, which is analytically pure and was provided by Shanghai Titan Reagent Co., Ltd. In this study, the detailed experimental scheme is shown in Table 3.

2.2. Methods

2.2.1. Sample Preparation. For each sample, 115 g dry sand particles were packed into a column. The grouting and solidification process of aeolian sand is carried out in a medical syringe. Other instruments mainly include balance, geononwoven fabric, labeled sand, funnel, beaker, purified water, tray, retainer, and peristaltic pump. The geononwoven fabric can make the $CaCO_3$ not block the grouting path and flow easily. The peristaltic pump can send the $CaCl_2$ to the sand, and the rotation speed is about 5 r/min.

The effects of different concentrations of $CaCl_2$, particle size distribution, and different grouting batches, respectively, are being studied.

2.2.2. Particle Size Distribution. The particle all-size distribution and particle size from 0.1 mm to 0.4 mm are selected under the premise of the basic scheme. As can be seen from Figure 3, the range from 0.1 mm to 0.4 mm of particle size is more particles in test. The particle size range that is too large (>0.4 mm) and too small (<0.1 mm) is removed.

2.2.3. Grouting Batches. Different grouting batches are selected including three times, four times, and five times to research. After the grouting and solidification are completed, the size of column is about 150 mm height and 50 mm

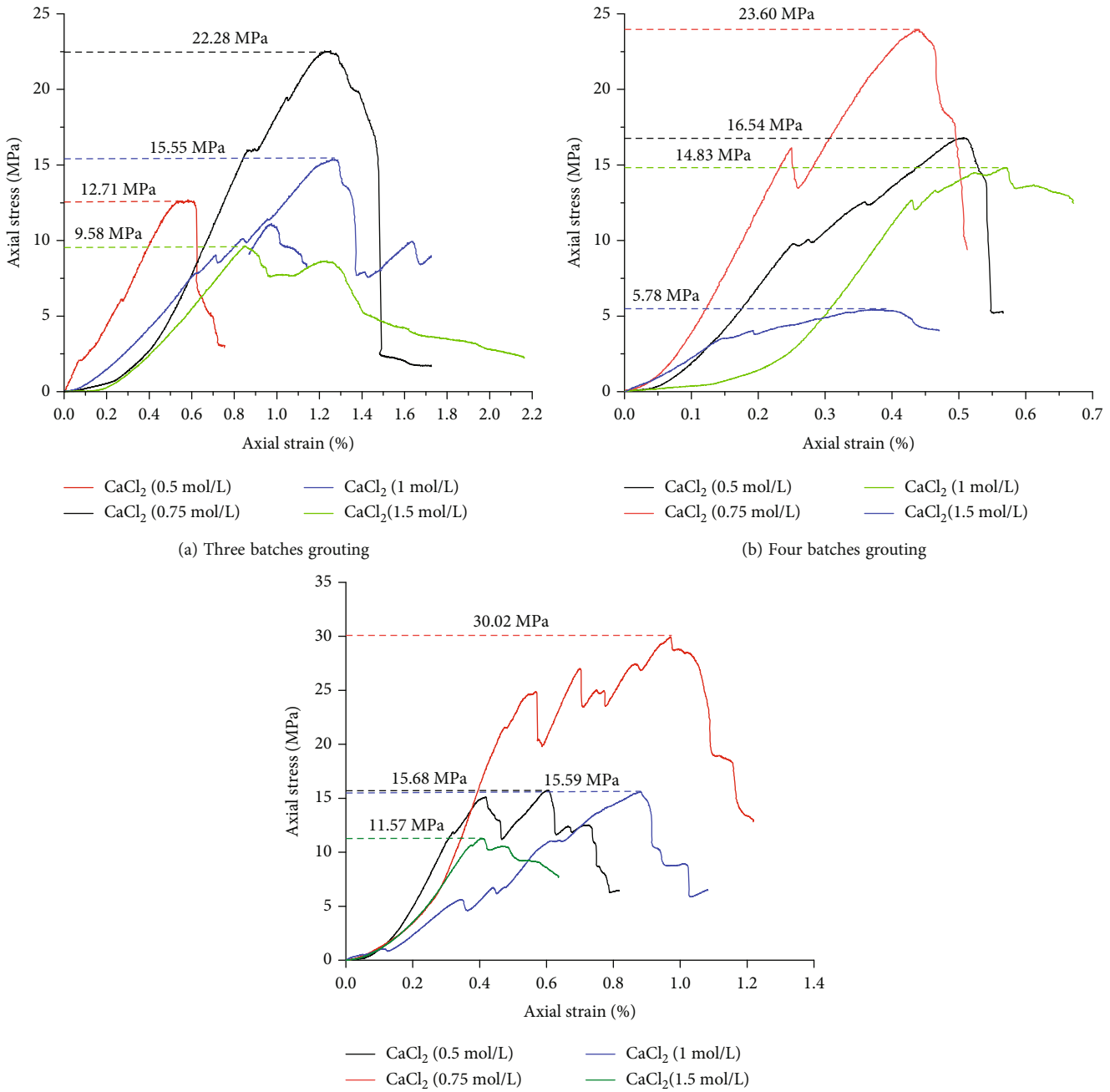

Figure 9: The representative stress-strain curves for UCS.

diameter. The syringe is divided into two parts with a tool, from which the aeolian sand column is taken out and labeled.

3. Results

3.1. Bender Element Test. The test uses the bender element BES in conjunction with the data acquisition system. Two size of probes are selected to measure the wave speeds for loose aeolian sand and solidified aeolian sand column, respectively, and the loose aeolian sand is to be the contrast one. The bender element shown in Figure 3.

The electromagnetic wave propagates through the piezoelectric ceramic plates at the ends of two probes of the bender element, one is the transmitting wave device, and the other one is the receiving wave device, completing a test cycle. The degree of different solidification aeolian sand is evaluated through measuring the speed of P-wave and S-wave. The process of measuring is shown in Figure 4.

As can be seen from Figure 2, neither P-wave nor S-wave continuously increases with the increase of nutrient concentration, but there is a peak value. When the concentration is 0.75 mol/L, the solidification of aeolian sand is better than other concentrations by using the MICP. The value for speed

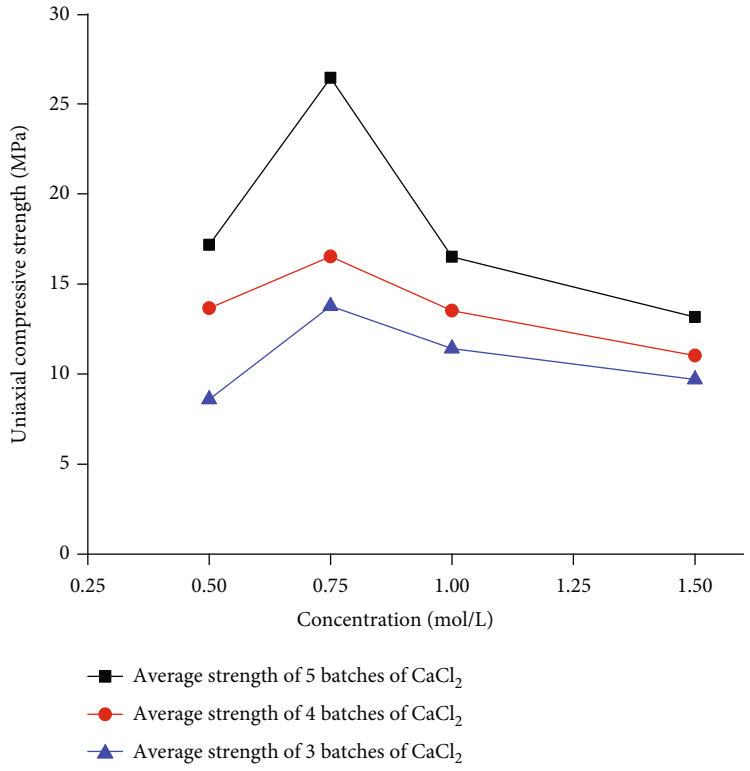

Figure 10: The uniaxial compressive strength in different batches.

of P-wave is bigger than that of the S-wave from the figure. As can be seen in Figure 5, the speed of P-wave is 1.3 times more than the speed of S-wave.

As can be seen in Figures 6 and 7, the wave speed of the particle all-size distribution is smaller than that of the particle size from 0.1 mm to 0.4 mm. The comparative test shows that the particle size is controlled in a relatively uniform range, which can make the pores between particles larger. $CaCO_3$ is much easier to cement, and the degree of cementation is much better.

There are three different kinds of nutrient concentrations to research, including 0.5 mol/L, 0.75 mol/L, and 1 mol/L. It can be seen from Figure 8 that under the same nutrient concentration, the largest wave speed of the grouting batches is the five batches, and the maximum is the 470 m/s, 550 m/s, and 500 m/s, respectively. It shows that grouting batches are beneficial to improve the solidification aeolian sand. Among the three different nutrient concentrations, the 0.75 mol/L has a relatively large S-wave speed, which is roughly distributed in the range of 450-550 m/s and the average value is higher than the other two concentrations. It also shows that when nutrient concentration is 0.75 mol/L, the aeolian sand solidification is much better.

The values of the P-wave and the S-wave which are tested in the bender element are all reasonable according to the standard for code for seismic design of buildings [38]. And the value of P-wave is one and a half times as large as S-wave.

3.2. UCS. The dried biocemented aeolian sand samples are cut into two parts (A and B); then, their surfaces are ground flat with a grinding machine to eliminate the influence of deviant stress in the compression process. The testing machine is MTS810, and the loading rate is 1 mm/min, controlled by the displacement. It records the process from loading to specimen failure, and the peak stress is the unconfined compressive strength of the specimen. Representative stress-strain curves are presented in Figure 9.

The UCS results are drawn in Figure 10. It can be seen that the UCS of biocemented aeolian sand samples increases when the concentration of cementation solution increases from 0.5 mol/L to 0.75 mol/L. However, when the concentration becomes larger than 0.75 mol/L, then UCS decreases. Additionally, the average value of UCS for the aeolian sand column increases along with the number of injections.

The trend of the UCS are reasonable compared with reference [31], moreover the figure is much more accurate.

3.3. SEM. The SEM images concerning crystal polymorph and microstructures of biocemented sand are presented. Compared with the loose sand particles presented, the aeolian sand particles after MICP treatment are covered by $CaCO_3$ crystals. It is found that the morphology of precipitated $CaCO_3$ crystals is mostly cubic. There are some round or slender rod-shaped holes showing on the $CaCO_3$ surfaces which are identified as the bacterial traces. The diameter of round holes is about 1micron, while the rod-shaped holes are 3-4 microns in length.

It is the precipitated $CaCO_3$ crystals acting as the cementitious materials which bond the loose sand particles together thus improving the mechanical properties of sand. With the increase of the grouting times, the living environment of microorganisms in the reaction system will be changed,

which is conducive to the attachment of microorganisms on the surface and joints of sand particles to form crystalline nuclei. It is also conducive to produce the $CaCO_3$ for increasing the sand strength.

Compared with four batches grouting, the amount of $CaCO_3$ crystals precipitated by five-batch injection with the same cementation solution concentration is much higher. As for the different concentrations, 0.75 mol/L can induce more $CaCO_3$ crystals than other concentrations, which corresponds to the figure where 0.75 mol/L can induce the highest UCS (26.09 MPa).

Compared with reference [23], the result of the SEM is similar to it. It is also confirmed that the result of the SEM is reasonable.

4. Conclusions

Based on the experimental results, the following conclusions can be drawn:

(1) Compared with the loose aeolian sand where the wave speed is only 200 m/s, the P-wave speed of biocemented aeolian sand column is about 450-600 m/s and the S-wave speed of it is about 350-500 m/s by the bender element test. It has been improved obviously, compared with loose aeolian sand with a wave speed of 200 m/s. All the values are reasonable according to the related standards

(2) This study investigated the effects of different concentrations of cementation solution. When the concentration of cementation solution is 0.75 mol/L, the speeds of P-wave and S-wave and the unconfined compression strength of biocemented aeolian sand are highest

(3) The best times of batches is five times, and the best nutrient concentration is 0.75 mol/L. The average of uniaxial compressive strength is 26.4 MPa under this condition. It is higher than that of four batches (16.51 MPa) and three batches (13.77 MPa). The results show that the solidification effect of aeolian sand is more much better based on MICP

(4) The reinforced aeolian sand has a dense microstructure and good compressive strength through SEM and UCS tests, which further indicates that the reinforced aeolian sand has high compressive strength

Data Availability

The data and materials are available.

Ethical Approval

All the authors declare that there is ethical approval.

Consent

Everybody consents to participate and to publish.

Disclosure

A preprint has previously been published [39].

Conflicts of Interest

The authors declare that they have no conflicts of interest.

Acknowledgments

This study is supported by Hebei Provincial Universities' Basic Scientific Research Operating Expenses (No. JQN2020027), the doctoral Research Initiation Fund of North China University of Science and Technology (No. 28418599), and Qing Dong Ling "National Cultural Relics Protection and Utilization Demonstration Zone" Construction Culture Research Project (QDLWHYJ0007).

References

[1] H. Kaltwasser, J. Krämer, and W. R. Conger, "Control of urease formation in certain aerobic bacteria," *Archives of Microbiology*, vol. 81, no. 2, pp. 178–196, 1972.

[2] S. Stocks-fischer, J. K. Galinat, and S. S. Bang, "Microbiological precipitation of $CaCO_3$," *Soil Biology and Biochemistry*, vol. 31, no. 11, pp. 1563–1571, 1999.

[3] P. L. A. Van, *Biogrout, ground improvement by microbial induced carbonate precipitation*, Delft University of Technology, 2009.

[4] A. Salwa, *High strength in-situ biocementation of soil by calcite precipitating locally isolated ureolytic bacteria*, Murdoch University, 2008.

[5] L. Cheng, R. Cord-ruwisch, and M. A. Shahin, "Cementation of sand soil by microbially induced calcite precipitation at various degrees of saturation," *Canadian Geotechnical Journal*, vol. 50, no. 1, pp. 81–90, 2013.

[6] Q. A. Al and K. Soga, "Effect of chemical treatment used in MICP on engineering properties of cemented soils," *Geotechnique*, vol. 63, no. 4, pp. 331–339, 2013.

[7] D. J. Tobler, E. Maclachlan, and V. R. Phoenix, "Microbially mediated plugging of porous media and the impact of differing injection strategies," *Ecological Engineering*, vol. 42, pp. 270–278, 2012.

[8] Y. Al-salloum, H. Abbas, and Q. I. Sheikh, "Effect of some biotic factors on microbially-induced calcite precipitation in cement mortar," *Saudi journal of biological sciences.*, vol. 24, no. 2, pp. 286–294, 2017.

[9] A. Mahawish, A. Bouazza, and W. P. Gates, "Effect of particle size distribution on the biocementation of coarse aggregates," *Acta Geotechnica*, vol. 13, no. 4, pp. 1019–1025, 2018.

[10] V. Ivanov and J. Chu, "Applications of microorganisms to geotechnical engineering for bioclogging and biocementation of soil in situ," *Reviews in Environmental Science and Biotechnology*, vol. 7, no. 2, pp. 139–153, 2008.

[11] M. P. Harkes, L. A. Van Paassen, J. L. Booster, V. S. Whiffin, and M. C. van Loosdrecht, "Fixation and distribution of bacterial activity in sand to induce carbonate precipitation for ground reinforcement," *Ecological Engineering*, vol. 36, no. 2, pp. 112–117, 2010.

[12] J. T. Dejong, M. B. Fritzges, and K. Nusslein, "Microbially induced cementation to control sand response to undrained

shear," *Journal of Geotechnical and Geoenvironmental Engineering*, vol. 132, no. 11, pp. 1381–1392, 2006.

[13] F. Ferris, L. Stehmeier, A. Kantzas, and F. M. Mourits, "Bacteriogenic mineral plugging," *Journal of Canadian Petroleum Technology*, vol. 36, no. 9, 1997.

[14] V. Achal, X. Pan, and Q. Fu, "Biomineralization based remediation of As (III) contaminated soil by Sporosarcina ginsengisol," *Journal of Hazardous Materials*, vol. 201-202, pp. 178–184, 2011.

[15] V. Achal, A. Mukherjee, and M. S. Reddy, "Microbial concrete: way to enhance the durability of building structures," *Journal of Materials in Civil Engineering*, vol. 23, pp. 730–734, 2010.

[16] M. G. Le, S. Castanier, and G. Orial, "Applications of bacterial of limestones in buildings and historic patrimony the protection and regeneration," *Sedimentary Geology*, vol. 126, pp. 25–34, 1999.

[17] C. Rodriguez-navarro, M. Rodriguez-gallego, and K. B. Chekroun, "Conservation of ornamental stone by Myxococcus xanthus-induced carbonate biomineralization," *Applied and Environmental Microbiology*, vol. 69, no. 4, pp. 2182–2193, 2003.

[18] W. D. Muynck, S. Leuridan, and D. V. Loo, "Influence of pore structure on the effectiveness of a biogenic carbonate surface treatment for limestone conservation," *Applied and Environmental Microbiology*, vol. 77, no. 19, pp. 6808–6820, 2011.

[19] D. V. Zamarreno, R. M. Inkpen, and E. May, "Carbonate crystals precipitated by freshwater bacteria and their use as a limestone consolidant," *Applied and Environmental Microbiology*, vol. 75, no. 18, pp. 5981–5990, 2009.

[20] K. Rowshanbakht, M. Khamehchiyan, R. H. Sajedi, and M. R. Nikudel, "Effect of injected bacterial suspension volume and relative density on carbonate precipitation resulting from microbial treatment," *Ecological Engineering*, vol. 89, pp. 49–55, 2016.

[21] N. K. Dhami, M. S. Reddy, and A. Mukheriee, "Significant indicators for biomineralisation in sand of varying grain sizes," *Construction and Building Materials*, vol. 104, pp. 198–207, 2016.

[22] S. Choi, K. Wang, and J. Chu, "Properties of biocemented, fiber reinforced sand," *Construction and Building Materials*, vol. 120, pp. 623–629, 2016.

[23] X. C. Xu, H. X. Guo, X. H. Cheng, and M. Li, "The promotion of magnesium ions on aragonite precipitation in MICP process," *Construction and Building Materials*, vol. 263, p. 120057, 2020.

[24] L. Cheng and R. Cord-Ruwisch, "In situ soil cementation with ureolytic bacteria by surface percolation," *Ecological Engincering*, vol. 42, pp. 64–72, 2012.

[25] W. W. K. Van, F. J. Vermolen, and M. G. A. M. Van, "Modelling biogrout: a new ground improvement method based on microbial-induced carbonate precipitation," *Transport in Porous Media*, vol. 87, pp. 397–420, 2011.

[26] W. W. K. Van, F. J. Vermolen, and M. G. A. M. Van, "A mathematical model and analytical solution for the fixation of bacteria in biogrout," *Transport in Porous Media*, vol. 92, no. 3, pp. 847–866, 2012.

[27] W. W. K. Van, F. J. Vermolen, and M. G. A. M. Van, "A mathematical model for biogrout," *Computational Geosciences*, vol. 17, no. 3, pp. 463–478, 2013.

[28] S. Fauriel and L. Laloui, "A bio-chemo-hydro-mechanical model for microbially induced calcite precipitation in soils," *Computers and Geotechnics*, vol. 46, pp. 104–120, 2012.

[29] D. Terzis and L. Laloui, "3-D micro-architecture and mechanical response of soil cemented via microbial-induced calcite precipitation," *Scientific Reports*, vol. 8, no. 1, p. 1416, 2018.

[30] X. H. Cheng, Z. Yang, and Z. C. Zhang, "Modeling of microbial induced carbonate precipitation in porous media," *Joumal of Pure and Applied Microbiology*, vol. 7, pp. 449–458, 2013.

[31] B. Li, *Geotechnical properties of biocement treated soils*, Nanyang Technological University, 2017.

[32] V. S. Whiffin, P. L. A. Van, and M. P. Harkes, "Microbial carbonate precipitation as a soil improvement technique," *Geomicrobiology Journal*, vol. 24, no. 5, pp. 417–423, 2007.

[33] B. C. Martinez, *Upscaling of Microbial Induced Calcite Precipitation in Sands for Geotechnical Ground Improvement*, Dissertations & Theses-Gradworks, 2012.

[34] P. L. A. Van, *Bio-mediatedground improvement: from laboratory experiment to pilot applications. Geo-Frontiers: Advances in Geotechnical Engineering*, ASCE, Dallas, 2011.

[35] D. S. W. R. L. Van and W. W. K. L. A. Van, *Stabilization of gravel deposits using microorganisms. Proceedings of the 15th European Conference on Soil Mechanics and Geotechnical Engineering*, IOS Press, Athens, 2011.

[36] P. L. A. Van, M. P. Harkes, and Z. A. Van, *Scale up of biogrout: a biological ground reinforcement method. Proceedings of the 17th International Conference on Soil Mechanics and Geotechnical Engineering. [S.l.]*, IOS Press, Lansdale, 2009.

[37] E. Kalkan, "A review on the microbial induced carbonate precipitation (MICP) for soil stabilization," *International Journal of Earth Sciences Knowledge and Applications*, vol. 2, no. 1, pp. 38–47, 2020.

[38] *Code for Seismic Design of Buildings*China Architecture & Building Press, GB 5011-2010, Beijing.

[39] Y. J. Zhou and H. T. Wang, "Experimental study on the aeolian sands solidification via MICP technique," https://www.researchsquare.com/article/rs-255149/v1.